N90-20552

Peter J. Melvin
Naval Research Laboratory, Washington, DC

Abstract

A new, geometrical, first order, nonresonant, frozen orbit theory has been developed based on Orlov's uniformly rotating plane of constant inclination. Perturbation spectra generated from a 90th order subset of OSU86F are shown for the ill-fated 1984 JHU/APL SAGE proposal for a pair of TRANSIT satellites at 400km altitude with a 93°.5 inclination.

## Introduction

To perform the integration for a geodetic satellite a new form has been developed for the geopotential on an orbit as

$$V = \frac{GM}{a} \sum_{k=0}^{\infty} \xi^k \sum_{p=-\infty}^{\infty} \sum_{q=-\infty}^{\infty} e^{i(pu + q\vartheta)} [\bar{R}^{(k)}_{p,q} + \varphi \bar{T}^{(k)}_{p,q}] ,$$

where the symbols are defined in [Melvin, 1988a] and an algorithm is derived for the generation of the complex coefficients from a spherical harmonic geopotential model.

The geopotential variation

$$a \sum_{p=-\infty}^{\infty} \sum_{q=-\infty}^{\infty} \bar{R}^{(0)}_{p,q} e^{i(pu+q\vartheta)} , \tag{1}$$

is the distance of an equipotential surface from sphere of radius a. The spectrum in Fig. 1 is a log-log bar graph of the amplitudes $2a|\bar{R}^{(0)}_{p,q}|$ where the frequency is $|pn + q\dot{\vartheta}|$. The along-track deflection evaluated on the nominal circular orbit is

$$\frac{1}{a}\frac{\partial V}{\partial u} = \frac{GM}{a^2} \sum_{p=-\infty}^{\infty} \sum_{q=-\infty}^{\infty} ip\bar{R}^{(0)}_{p,q} e^{i(pu+q\vartheta)} , \tag{2}$$

and its spectrum is plotted in Fig. 2.

## Position Perturbations

The real forms of the series are used for the integration in [Melvin 1988a], but it is apparent from [Melvin, 1988b] that the formulas are much simpler with complex coefficients. In fact the orbit perturbations are of the same form as the disturbing potential

$$\varphi = \sum_{p=-\infty}^{\infty} \sum_{q=-\infty}^{\infty} \varphi_{p,q} e^{i(pu+q\vartheta)} , \qquad \eta = \sum_{p=-\infty}^{\infty} \sum_{q=-\infty}^{\infty} \eta_{p,q} e^{i(pu+q\vartheta)} ,$$

$$\xi = \sum_{p=-\infty}^{\infty} \sum_{q=-\infty}^{\infty} \xi_{p,q} e^{i(pu+q\vartheta)} , \qquad \chi = \sum_{p=-\infty}^{\infty} \sum_{q=-\infty}^{\infty} \chi_{p,q} e^{i(pu+q\vartheta)} ,$$

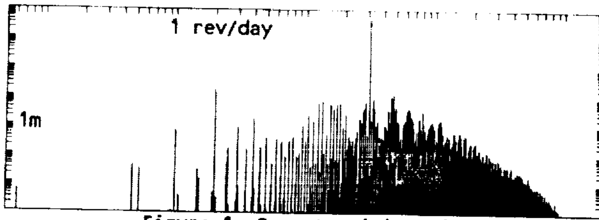

Figure 1. Geopotential Variation

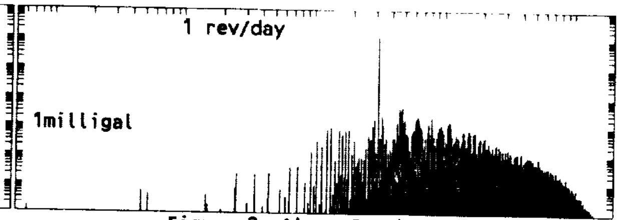

Figure 2. Along-Track Deflection

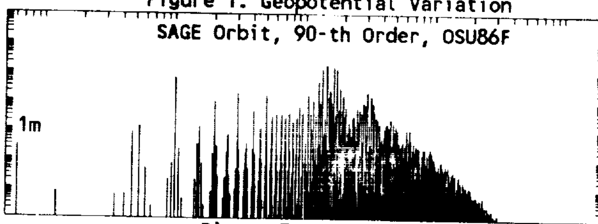

Figure 3. Cross-Track

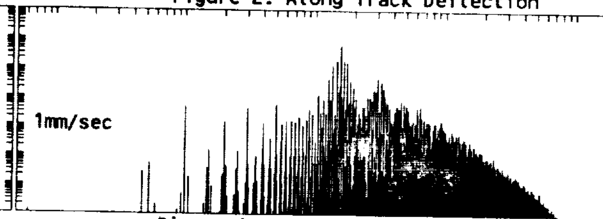

Figure 4. Cross-Track Velocity

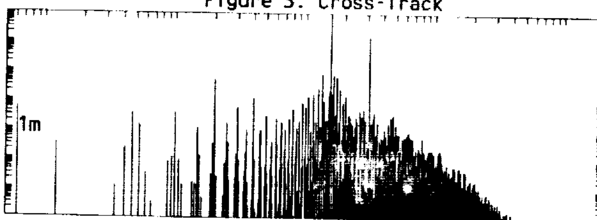

Figure 5. Radial

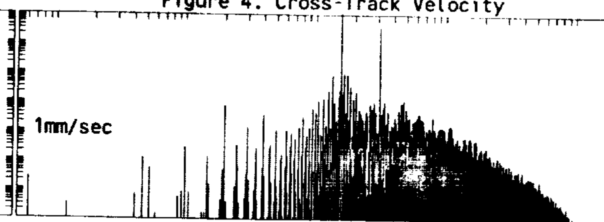

Figure 6. Radial Velocity

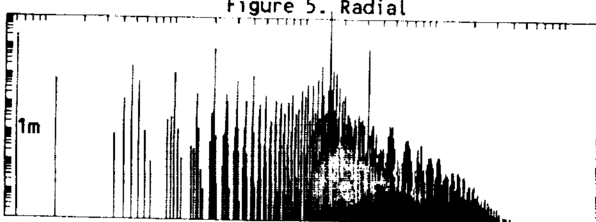

Figure 7. Along-Track

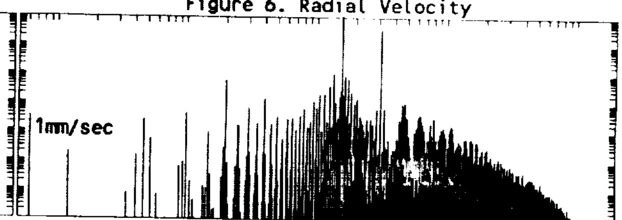

Figure 8. Along-Track Velocity

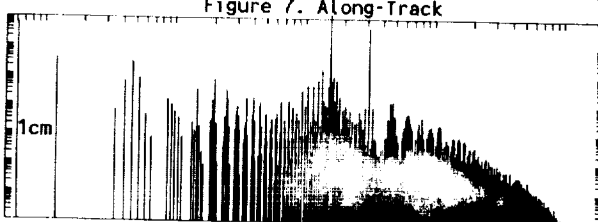

Figure 9. Intersatellite Range

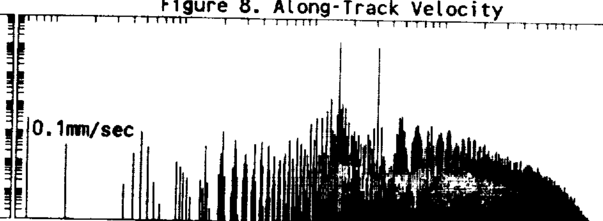

Figure 10. Intersatellite Range-Rate

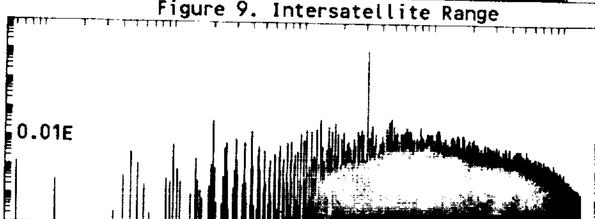

Figure 11. Radial, Radial Gravity Gradient

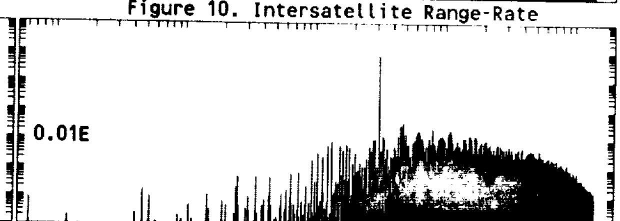

Figure 12. Radial, Along Gravity Gradient

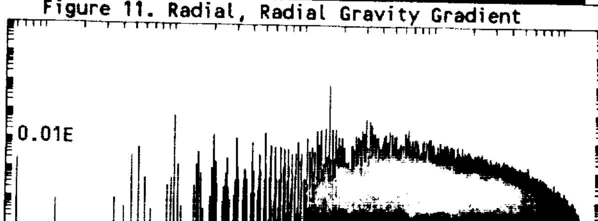

Figure 13. Radial, Cross Gravity Gradient

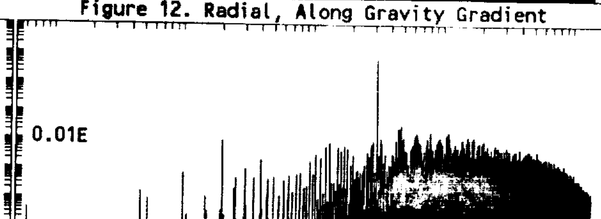

Figure 14. Along, Along Gravity Gradient

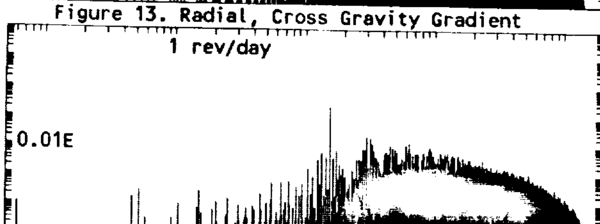

Figure 15. Along, Cross Gravity Gradient

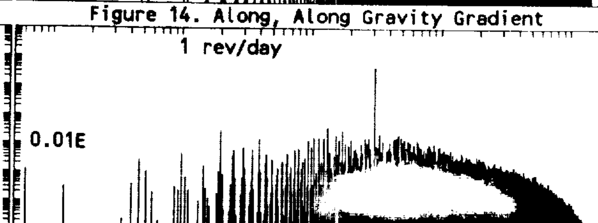

Figure 16. Cross, Cross Gravity Gradient

where the coefficients are computed from the algorithm

$$\varphi_{p,q} = -\frac{n_o^2 \overline{T}^{(0)}_{p,q}}{(pn+q\dot{\vartheta})^2 - N^2} \quad , (3), \qquad \eta_{p,q} = \frac{n_o^2 p \overline{R}^{(0)}_{p,q}}{\nu(pn+q\dot{\vartheta})} \ ,$$

$$\xi_{p,q} = -\frac{n_o^2 \overline{R}^{(1)}_{p,q} + 2\nu^2 \eta_{p,q}}{(pn+q\dot{\vartheta})^2 - N^2} \ , (5), \qquad \chi_{p,q} = -i\nu \frac{\eta_{p,q} - 2\xi_{p,q}}{pn + q\dot{\vartheta}} \ . \tag{7}$$

After multiplication by 2a, the amplitudes of the coefficients of (3), (5) and (7) are plotted in Figs. 3, 5, and 7 from which it is seen that position perturbations accentuate the low and near orbital frequencies and attenuate the high frequencies. Expressions for the cross-track (3), radial (5), and along-track (7) position perturbations from the Kaula-Allan theory are found in [Rosborough and Tapley, 1987].

## Velocity Perturbations

By use of coordinates at the nominal satellite position, the cross-track, radial, and along-track velocity components are

$$v_\varphi = a(\dot{\varphi} - \dot{\Omega}\sin\iota\cos u) = a[\sum_{p=-\infty}^{\infty} \sum_{q=-\infty}^{\infty} i(pn+q\dot{\vartheta})\varphi_{p,q} e^{i(pu+q\vartheta)} - \dot{\Omega}\sin\iota\cos u] , \tag{4}$$

$$v_r = a\dot{\xi} = a \sum_{p=-\infty}^{\infty} \sum_{q=-\infty}^{\infty} i(pn + q\dot{\vartheta})\xi_{p,q} e^{i(pu+q\vartheta)} \ , \tag{6}$$

$$v_u = a\nu + a(\dot{\chi} + \nu\xi) = a\nu[1 + \sum_{p=-\infty}^{\infty} \sum_{q=-\infty}^{\infty} (\eta_{p,q} - \xi_{p,q}) e^{i(pu+q\vartheta)}] \ . \tag{8}$$

The amplitudes of the coefficients of (4), (6) and (8) are plotted in Figs. 4, 6, and 8. By comparison of the high frequency fall-off in the position and velocity spectra, it is clear why more geopotential information is obtained from Doppler beacon satellites than from skin tracking even if it is by laser reflectors.

## Intersatellite Measurements

For a close satellite pair in same orbit, the intersatellite range is

$$\rho = r\Delta u = a\delta u(1 + \xi + \frac{\partial \chi}{\partial u}) = a\delta u[1 + \sum_{p=-\infty}^{\infty} \sum_{q=-\infty}^{\infty} (\xi_{p,q} + ip\chi_{p,q}) e^{i(pu+q\vartheta)}] , \tag{9}$$

A time derivative yields the intersatellite range rate as

$$\dot{\rho} = a\delta u \sum_{p=-\infty}^{\infty} \sum_{q=-\infty}^{\infty} i(pn + q\dot{\vartheta})(\xi_{p,q} + ip\chi_{p,q}) e^{i(pu+q\vartheta)} \ . \tag{10}$$

For a nominal separation of $a\delta u$=100km the spectra of (9) and (10) are plotted in Figs. 9 and 10. A comparison of the high frequency portions of Figs. 2 and 10 and the foregoing formulas show

$$\dot{\rho} \simeq \frac{a\delta u}{a^2 n} \frac{\partial V}{\partial u} \ ,$$

from which the result of [Comfort, 1973] is modified to state that at high frequencies for a pair of satellites flying in formation the intersatellite range rate mimics the along track deflection. The paucity of spectral lines near twice per orbit in Fig. 10 indicates that complete geopotential recovery is not possible with only intersatellite range rate.

## Gravity Gradient

Equally simple formulas for the gravity gradient tensor along a nominal circular orbit in Orlov's plane are found in [Melvin, 1988b] as

$$\Gamma_{r,r} = 2n_o^2 \sum_{p=-\infty}^{\infty} \sum_{q=-\infty}^{\infty} \bar{R}_{p,q}^{(2)} e^{i(pu+q\vartheta)} \quad (11), \qquad \Gamma_{r,u} = in_o^2 \sum_{p=-\infty}^{\infty} \sum_{q=-\infty}^{\infty} p(\bar{R}_{p,q}^{(1)} - R_{p,q}^{(0)}) e^{i(pu+q\vartheta)}, \quad (12)$$

$$\Gamma_{r,\varphi} = n_o^2 \sum_{p=-\infty}^{\infty} \sum_{q=-\infty}^{\infty} (\bar{T}_{p,q}^{(1)} - \bar{T}_{p,q}^{(0)}) e^{i(pu+q\vartheta)} \quad (13), \qquad \Gamma_{u,u} = n_o^2 \sum_{p=-\infty}^{\infty} \sum_{q=-\infty}^{\infty} (-p^2 \bar{R}_{p,q}^{(0)} + \bar{R}_{p,q}^{(1)}) e^{i(pu+q\vartheta)}, \quad (14)$$

$$\Gamma_{u,\varphi} = in_o^2 \sum_{p=-\infty}^{\infty} \sum_{q=-\infty}^{\infty} p\bar{T}_{p,q}^{(0)} e^{i(pu+q\vartheta)} \quad (15), \qquad \Gamma_{\varphi,\varphi} = -\Gamma_{r,r} - \Gamma_{u,u} \,. \quad (16)$$

The gravity gradient spectra computed from (11) through (16) are shown in Figs. 11 through 16.

## Geopotential Recovery

Although it is subjective and dependent on the sensitivity of the measuring devices, it became apparent in the generation of the spectrum in Fig. 10 that the claim of 100th order recovery from SAGE, [Pisacane, et al., 1984], could not be substantiated. From intersatellite range rate, about 70th order recovery is more realistic at an altitude of 400km. The abrupt, high frequency cutoff in Figs. 11, 12, and 14 indicates there is information beyond 90th order in the gravity gradient components.

## References


Comfort, G.C., "Direct Mapping of Gravity Anomalies by Using Doppler Tracking between a Satellite Pair", J. Geophys. Res., *78*, 6845, 1973

Melvin, P.J., "Satellite Geodesy from Orlov's Plane", (AAS 87-536), Advances in the Astronautical Sciences, eds. Soldner, Misra, Lindberg and Williamson, *65*, 1449, 1988a

Melvin, P.J., "The figure-of-8 librations of the gravity gradient pendulum and modes of an orbiting tether: II. Geodetic, mass distribution and eccentricity effects", AIAA 88-4283-CP, Proc. AIAA/AAS Astrodynamics Conference, Minneapolis, MN, p 503, 1988b

Pisacane, V.L., Yionoulis, S.M., Eisner, A., and Black, H.D., "SAGE - A Two Satellite Experiment for Improving the Gravity Model", EOS, *65*, 858, 1984

Rosborough, G.W., and Tapley, B.D., "Radial, Transverse and Normal Satellite Position Perturbations Due to the Geopotential", Celestial Mechanics, *40*, 409, 1987